Available online at website: https://journal.bcrec.id/index.php/bcrec

Bulletin of Chemical Reaction Engineering & Catalysis, 20 (3) 2025, 505-516

Original Research Article

Strategic Synthesis of Hierarchical Co_3O_4/ZSM-5 Zeolite as A Catalyst in Partial Oxidation of Methane: Bottom-up vs Top-down Methods

Irena Khatrin[1,2,§], Danika Nurranalya Putri[1,2,§], Muhammad Ridwan[1], Yuni Krisyuningsih Krisnandi[1,2,*]

[1]Department of Chemistry, Faculty of Mathematics and Natural Sciences, Universitas Indonesia, Kampus UI Depok, Depok 16424, Indonesia
[2]Solid Inorganic Framework Laboratory, Department of Chemistry, Faculty of Mathematics and Natural Sciences, Universitas Indonesia, Kampus UI Depok, Depok 16424, Indonesia

Received: 12th July 2025; Revised: 30th July 2025; Accepted: 31th July 2025
Available online: 18th August 2025; Published regularly: October 2025

Abstract

Methane, a potent greenhouse gas contributing approximately 19% to global warming and possessing a global warming potential 28 times greater than carbon dioxide, necessitates conversion into more beneficial chemicals. Partial oxidation of methane to methanol is a promising conversion method which is both time- and cost-efficient. This study synthesized ZSM-5 using two strategic syntheses: Bottom-Up and Top-Down, followed by cobalt oxide impregnation at varying percentages 2.5, 5, and 10% (w/w) to produce Co_3O_4/ZSM-5. To investigate its physicochemical properties, ZSM-5 catalysts were thoroughly characterized with XRD, FTIR, XRF, N_2-physisorption, and SEM. These catalysts were then evaluated in methane partial oxidation reactions conducted in a batch reactor, with a CH_4:N_2 feed ratio of 0.75 bar:2 bar, at 150 °C for 60 minutes. Co_3O_4-supported Bottom-Up ZSM-5 with 5% Co-loading demonstrated the largest percentage yield of 62.08% compared to the other Co-loading amount and ZSM-5 synthesized via Top-Down method.

Keywords: Hierarchical ZSM-5; Co_3O_4; Bottom-up; Top-down; Partial Oxidation of Methane

How to Cite: Khatrin, I., Putri, D. N., Ridwan, M., Krisnandi, Y. K. (2025). Strategic Synthesis of Hierarchical Co_3O_4/ZSM-5 Zeolite as A Catalyst in Partial Oxidation of Methane: Bottom-up vs Top-down Methods. *Bulletin of Chemical Reaction Engineering & Catalysis*, 20 (3), 505-516. (doi: 10.9767/bcrec.20441)

Permalink/DOI: https://doi.org/10.9767/bcrec.20441
Supporting Information (SI): https://journal.bcrec.id/index.php/bcrec/article/downloadSuppFile/20441/5815

1. Introduction

Climate change has become a key global concern, encompassing the phenomenon of global warming, characterized by a rise in the average surface temperature of earth. This trend is primarily driven by increased concentration of greenhouse gases including carbon dioxide (CO_2), nitrous oxide (N_2O), and methane (CH_4). Unlike stable atmospheric components like nitrogen (N_2) and oxygen (O_2), these gases have the capacity to absorb and re-emit infrared radiation, giving the warming effect towards earth [1,2]. A particularly potent greenhouse gas, methane, accounts for around 19% of global warming and is 28 times more potent than carbon dioxide for over a century [3]. Converting this abundant methane into useful fine chemicals offers a promising approach to both mitigate greenhouse gas emissions and create valuable chemical products. Historically, methanol production relied on indirect syngas routes, which are capital and operationally intensive, making them suitable only for large-

* Corresponding Author.
Email: yuni.krisnandi@sci.ui.ac.id (Y. K. Krisnandi)
§ Both authors contributed equal amount of work.

scale operations [4]. However, the direct conversion methods are more compact, cost-effective, and also offer higher conversion and selectivity at smaller scales [5].

In the early stages of Partial Oxidation of Methane (POM) catalyst development, various metal oxide-based catalysts, such as MoO_3-based [6], VO_x-based [7], and Fe_2O_3-based catalysts [8] were extensively employed. While metal oxide-based catalysts showed initial promise, they often suffered from significant drawbacks, including a high tendency for complete oxidation of methane to undesirable CO_2, and a selectivity bias towards formaldehyde [9]. Furthermore, these metal oxide catalysts often exhibit a propensity for metal oxide agglomeration at high temperatures, leading to a reduction in active surface area and consequently, a decrease in catalytic efficiency during POM reactions [10]. These limitations have prompted a search for more efficient and selective catalytic systems, one of them being the addition of support material, which plays a pivotal role in promoting the dispersion of active sites and influencing reaction pathways. Mesoporous silica [11], mesoporous carbon [12], and various types of zeolites have been extensively investigated [13,14]. Among these, metal-supported zeolites have emerged as a more favored alternative due to their tunable acidity, well-defined pore structure, and enhanced selectivity towards methanol. Crucially, the effectiveness of these metal-supported catalysts highly depends on the uniform dispersion of metal active sites across the surface of the support material. Good metal dispersion maximizes the accessibility of reactants to the active sites, thereby improving catalytic efficiency and preventing premature deactivation through agglomeration [15].

Within this context, ZSM-5 zeolite has consistently demonstrated exceptional catalytic performance in the POM reaction. For instance, Michalkiewicz *et al.* explored the POM reaction producing methanol and formaldehyde using oxygen over modified Fe-ZSM-5, reporting the highest methane conversion with Fe-HZSM-5 [16]. Subsequently, Beznis *et al.* investigated the POM reaction using Co-supported microporous ZSM-5, noting that the metal preparation route significantly influenced cobalt species behavior and, consequently, product selectivity, with impregnated Co-ZSM-5 favoring methanol production over formaldehyde [17]. Building on these findings, and in contrast to Co-supported microporous ZSM-5, our research group (2015) demonstrated that hierarchical Co-ZSM-5 prepared via impregnation produced a better methane conversion [18]. Furthermore, recent research by our research group has continued to explore the influence of the mesoporous configuration of hierarchical ZSM-5 on its catalytic performance in the POM reaction [19]. The optimum methane conversion and improved catalytic lifetime were shown by Co_3O_4 impregnated into hierarchical ZSM-5 with intracrystalline type of mesoporous, which exhibited selectivity for methanol as the main product [19].

Hierarchical ZSM-5 could be achieved via two primary synthesis routes: (a) the bottom-up approach, which involves hydrothermal modifications using various templates (hard or soft) and, (b) the top-down approach, which involves post-synthesis treatments such as dealumination or desilication. Exploring both synthesis methodologies is crucial because they inherently lead to distinct structural and textural properties in the resulting hierarchical ZSM-5. These differences include varied pore architecture, acidity, and surface area [20], which can significantly influence the catalytic performance of the as-synthesized zeolite in the POM reaction. By investigating both-bottom-up and top-down strategies, a more comprehensive understanding of how synthesis pathway dictates catalytic efficiency for methane partial oxidation can be obtained, allowing for a more informed selection or design of optimal catalyst systems.

Therefore, this study investigated the two distinct methods to synthesize hierarchical ZSM-5. The bottom-up method employed a dual-templates approach (TPAOH and PDDA-Cl), while the top-down method utilized desilication treatment using NaOH solution on a pre-synthesized microporous ZSM-5 framework. The as-synthesized ZSM-5 catalysts were then modified with Co-oxide with varied Co-loading (%) and characterized using a series of instrumentations to investigate their physicochemical properties. Furthermore, POM reactions was applied with varied reactions times to assess the differences in product yield and achieve the optimal reaction conditions.

2. Materials and Methods

2.1. Materials

Tetraethyl orthosilicate (TEOS, 98%), sodium aluminate ($NaAlO_2$), tetrapropylammonium hydroxide (TPAOH, 40 wt.%), poly(diallyldimethylammonium) chloride (PDDA-Cl, 20 wt.%), and ethanol were acquired from Sigma Aldrich. Acetic acid (glacial, 100%, for analysis), cobalt(II) nitrate hexahydrate ($Co(NO_3)_2 \cdot 6H_2O$), and sodium hydroxide (pellets) were acquired from Merck. CV Retno Gas supplied the Ultra High Purity (UHP) grade gases used in the experiment, including methane and nitrogen with 0.5% O_2. Deionized water and all other compounds were of reagent grade and used without any prior purifying procedures.

2.2. Synthesis of Hierarchical ZSM-5 Catalyst

2.2.1. Bottom-up Method

The bottom-up synthesis of hierarchical ZSM-5 was conducted according to the reported route of our research group [19]. This method employed TPAOH and PDDA-Cl as co-templates, with $NaAlO_2$ and TEOS serving as the respective Al and Si precursors. At 100 °C, these precursors were combined in the following molar ratio: 1.0 Al_2O_3 : 64.3 SiO_2 : 10.1 $(TPA)_2O$: 3571.7H_2O. The pH of the mixture was then adjusted to 11 using acetic acid. Following 48 h of stirring and room temperature storage, the homogeneous mixture was moved to an autoclave lined with Teflon and crystallized in an oven at 170 °C for 144 h. The resulting precipitate was filtered, washed to neutral, dried, and then calcined in static air at 550 °C for 3 h to produce hierarchical ZSM-5, which denoted as ZBU.

2.2.2. Top-down Method

The top-down method was also carried out following the synthesis procedure of our research group [18], as modified from Ogura *et al.* [21]. Prior to the synthesis of hierarchical ZSM-5, microporous ZSM-5 (ZM) was synthesized following the procedure of ZBU synthesis without the addition of secondary template PDDA-Cl. The as-synthesized ZM was then mixed with 0.2 M NaOH solution (1 g ZM to 300 mL NaOH) for 30 min under stirred reflux condition. The mixture was then transferred into an ice bath directly. The resulting precipitate was filtered, washed to neutral, and dried. Hierarchical ZSM-5 produced using this method was denoted as ZTD.

2.3. Co-oxide Impregnation

Co-oxide was incorporated into the as-synthesized ZSM-5 via impregnation method based on the technique reported by researcher [22]. A 0.25 M Co-precursor solution was added with a varied Co-to-ZSM-5 support ratio of 2.5, 5, and 10%. The mixture was agitated at room temperature, dried, and followed by calcination under static air condition at 550 °C for 3 h. Co-oxide impregnated ZSM-5 catalysts were denoted as *x*Co/ZBU and *x*Co/ZTD, where '*x*' represents the Co-loading percentage (2.5, 5, and 10% w/w) on the ZSM-5 support.

2.4. Catalyst Characterization

An Empyrean X-ray diffractometer from PANalytical was utilized for structural and crystallinity assessments, operating at 40 kV and 30 mA with Cu-Kα radiation (λ = 1.54059 Å) for scans within the 2θ range of 5–50°. Identification of functional groups was carried out using an Alpha-Bruker Fourier Transform Infrared (FTIR) spectrometer, applying the KBr pellet method technique to obtain spectra at 4 cm^{-1} resolution. Elemental composition was determined by X-Ray Fluorescence (XRF) analyses, performed on a PANalytical ϵ1 instrument (50 kV, Ag radiation). Furthermore, N_2-physisorption (at 77 K) provided insight into surface area and porosity with measurements conducted on a Quantachrome Quadrasorb-Evo analyzer. Before analysis, samples underwent degassing at 300 °C. The specific surface area, micropore volume, and Pore Size Distribution (PSD) was quantified using the Brunauer–Emmett–Teller (BET), the t-plot, and Barrett–Joyner–Halenda (BJH) method from the desorption branch, respectively. Total pore volume was derived from the amount of N_2 adsorbed at relative pressure (p/p_0) of 0.99. Quantachrome NovaWin – Data Acquisition and Reduction software facilitated the whole N_2-physisorption data analysis. Finally, sample surface morphology was examined using a JEOL JSM-6510LA Scanning Electron Microscopy (SEM) instrument.

2.5. Catalytic Test

Partial Oxidation of Methane (POM) reactions were conducted in a batch reactor at 150 °C using 0.5 g of catalyst. Initially, the reactor was flushed with N_2 gas for 10 min to eliminate impurities, while catalyst underwent activation treatment at 550 °C for 1 h. Subsequently, 0.75 bars of CH_4 and 2 bars of N_2 were simultaneously introduced into the reactor for 10 min. The reactor was then heated to 150 °C for 60 minutes of reaction time. Following the catalytic tests, the products adsorbed on the catalyst were extracted using 3 mL of ethanol. The products were separated from the catalyst by centrifugation at 4000 rpm for 4 minutes at room temperature. A 1 µL sample was injected into a Shimadzu FID-2014 Gas Chromatography (GC) instrument with an RTX-1 carbowax column and a flame ionization detector.

3. Results and Discussion

3.1. Catalyst Characterization

Figure 1 displayed the XRD patterns of both the as-synthesized hierarchical ZSM-5 catalysts and their Co-oxide modified counterparts. The pristine ZBU and ZTD catalysts showed characteristic peaks aligning with the MFI reference at 2θ values of 7.9, 8.9, 23.2, 24.0, and 24.5°. These peaks correspond to the (101), (020), (051), (151), and (303) planes of the MFI framework, respectively, as confirmed by JCPDS 44–0003 [23,24]. The relative crystallinity was assessed by analyzing the intensity of peaks within 2θ range of 21–26, following the ASTM D5758-01 method [25,26]. Notably, ZBU sample

synthesized via dual-templating method exhibited the highest intensity in its XRD pattern, thus serving as a reference with 100% relative crystallinity. These findings indicate that the synthesis of the hierarchical component of ZTD under alkaline conditions, which aimed at pore opening via desilication/dealumination, was accompanied by a reduction in the crystallinity of the resulting zeolite framework. This partial detriment to the ZSM-5 framework suggests a trade-off between increased mesoporosity and maintaining structural integrity during the alkaline treatment [27].

After the incorporation of Co-oxide, the structure of Co-derived ZBU and ZTD samples were preserved, as shown by the consistent presence and integrity of the characteristic ZSM-5 peaks in the XRD patterns. In addition, Co-incorporation resulted in the appearance of new peak at 2θ = 36.8°, corresponding to (311) planes of Co_3O_4 with spinel structure (JCPDS 42–1467) [28]. On the other hand, Co_3O_4 incorporation was observed to reduce the relative crystallinity of pristine ZBU and ZTD as the Co_3O_4 ratio increased, with better crystallinity preserved by ZBU samples compared to ZTD [29,30]. Furthermore, peak shifting was noted for ZBU, ZTD, and their Co_3O_4-derivatives. Specifically, ZBU samples exhibited a shift towards smaller 2θ values, while ZTD samples generally showed a shift towards larger 2θ values. This difference in peak shifting could be attributed to variations in lattice parameters or microstrain induced by distinct synthesis pathways and the specific distribution of Co species within the zeolite frameworks, without changing the overall structure [31].

FTIR spectra of pristine ZBU and ZM samples (Figure S1), where ZM served as the precursor for ZTD synthesis, were investigated to confirm the successful removal of the Organic Structure Directing Agent (OSDA) template utilized in the synthesis process. FTIR spectra prior to calcination displayed absorption peaks at 2980 cm^{-1} and 1467 cm^{-1}, attributed to C–H bending vibrations of OSDA template [32]. Notably, these absorptions were absent in the ZSM-5 samples after calcination, indicating that the calcination process as 550 °C successfully decomposed the TPAOH and PDDA−Cl templates in both ZM and ZBU, respectively. Furthermore, FTIR spectra of ZBU, ZTD, and their Co-derivatives are presented in Figure 2, while the clear stacked FTIR spectra are presented in Figure S2. All catalysts display five characteristic peaks of zeolite between 1600 and 500 cm^{-1}. Peaks at 1220 cm^{-1} are attributed to the asymmetric stretching modes, whilst the peaks at 1105 cm^{-1} and 800 cm^{-1} are assigned to the external symmetric stretching modes of T–O–T linkages (where T represents Si or Al within TO_4 tetrahedra) [33,34]. Furthermore, peak at 555 cm^{-1} correspond to the vibrational mode of distorted double five-membered rings (DDR5) characteristic of ZSM-5 [35,36].

Adsorbed H_2O is responsible for an absorption peak at 1630 cm^{-1} [37]. Broad peaks spanning 4000–3000 cm^{-1} indicate stretching vibrations from silanol (Si–OH) groups. ZBU catalysts exhibit two distinct peaks at 3630 and 3440 cm^{-1}, suggesting the coexistence of both isolated and hydrogen-bonded silanol groups [38]. Al–OH groups that are Brønsted acid sites and reside inside the ZSM-5 framework may also be responsible for the peak at 3440 cm^{-1} [39]. In contrast, the corresponding peak in ZTD samples primarily consists of hydrogen-bonded silanol groups. However, it should be noted that further characterization needs to be employed to confirm these results.

Additionally, the spectra of both ZBU and ZTD demonstrated the appearance of two new peaks after Co_3O_4 incorporation, specifically at 670 cm^{-1} and 600 cm^{-1}. These new peaks are

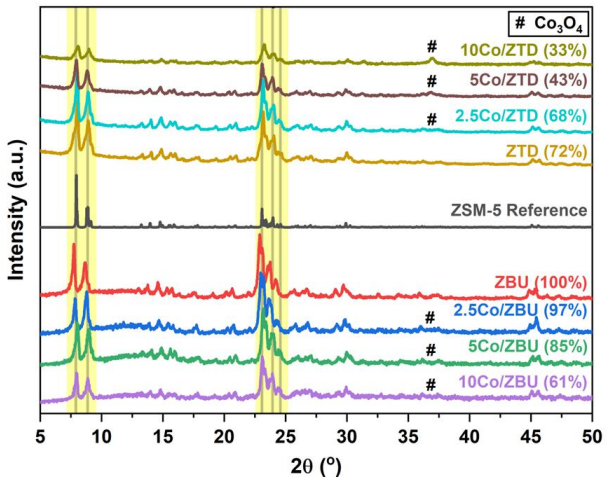

Figure 1. XRD patterns of ZBU, ZTD, and their Co_3O_4-derivatives (inset relative crystallinity).

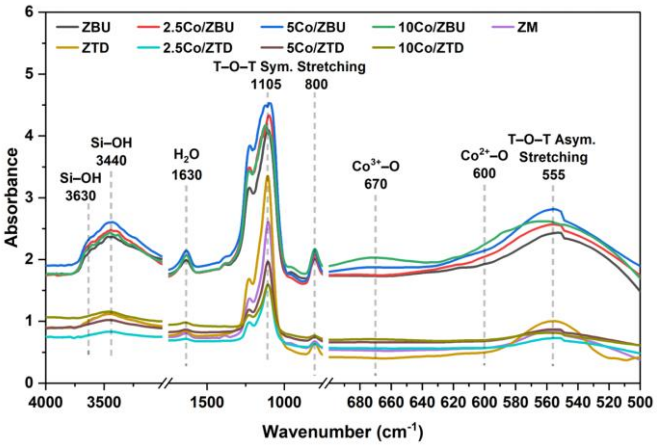

Figure 2. FTIR spectra of ZBU, ZTD, and their Co_3O_4-derivatives.

attributed to the stretching vibrations of Co^{3+}–O and Co^{2+}–O species, characteristic of Co_3O_4 spinel consisting of both Co(III) and Co(II) in its framework [5,40]. Consistent with the XRD observations, the intensity of these new peaks increased proportionally with higher metal loading.

XRF analysis in Table 1 provides insight into the elemental composition of the as-synthesized catalysts. The pristine ZBU and ZTD samples initially exhibited Si/Al ratios of 53 and 51, respectively. However, the subsequent incorporation of Co-oxide led to discernible changes in these ratios. For ZBU-derived catalysts, the Si/Al ratio decreased to values ranging from 39 (for 5Co/ZBU and 10Co/ZBU) to 41 (for 2.5Co/ZBU). A more substantial reduction in Si/Al ratio was observed for ZTD-derived samples, ranging from 12 (for 2.5Co/ZTD) to 23 (for 5Co/ZTD and 10Co/ZTD). These shifts indicate an alteration in the framework composition during the modification process.

Regarding the actual Co_3O_4 content, XRF confirmed the successful metal deposition. The measured Co loadings (w/w) were 3% for 2.5Co/ZBU and 2.5Co/ZTD, 8% for 5Co/ZBU, 9% for 5Co/ZTD, 16% for 10Co/ZBU, and 18% for 10Co/ZTD. These actual metal loadings are in good agreement with their respective theoretical Co values, confirming effective cobalt incorporation into the hierarchical ZSM-5 structures.

The textural and surface characteristics of the as-synthesized ZSM-5 catalysts and their Co_3O_4-derivatives were examined using N_2-physisorption (Table 1). The adsorption-desorption isotherms obtained for all samples consistently exhibited a Type IV isotherm with a hysteresis loop at relative pressure (p/p_0) > 0.4, indicating capillary condensation within mesopores [41]. These results confirm the successful introduction of secondary porosity in the size of mesopore (2–50 nm) to create hierarchical ZSM-5. The presence of parallel adsorption and desorption branches further indicates an open mesoporous system, well connected to the external surface of hierarchical ZSM-5 [42]. Furthermore, all catalysts were observed to exhibit an H4-type hysteresis loop, characterized by a gradual increase in the adsorption-desorption curve, which suggests the formation of silt-shaped pores with relatively small sizes (approx. 2 nm) [43]. These results are in agreement with similar method reported by Oktaviani *et al*. [44]. Moreover, the isotherms of both ZBU and ZTD samples after Co-incorporation exhibited similar profiles to their pristine counterparts, reinforcing the XRD findings that the impregnation process did not significantly alter the structural integrity of hierarchical ZSM-5 framework [45].

Analysis using the t-plot method confirmed the hierarchical pore distribution, providing specific values for micropore (S_{micro}) and external (S_{ext}) surface areas. The pristine ZBU (417 m^2/g) catalyst synthesized via dual-templating method showed a higher BET surface area (S_{BET}) compared to the ZM (399 m^2/g) and pristine ZTD catalyst (382 m^2/g).

Furthermore, since hierarchical counterparts in ZSM-5 are crucial for efficient mass transport and its use as a catalyst in POM reaction, Indexed Hierarchy Factor (IHF) shown in Table 1 (Eq. 1), was determined to quantify the hierarchical characteristics by taking into account the amounts of microporous and external porosity [46,47].

Table 1. Compositional and textural properties of ZBU, ZTD, and their Co_3O_4-derivatives. [a]Determined using BET method; [b]Determined using t-plot method; [c]Determined at $p/p_0 = 0.99$; [d]Determined using BJH.

Catalyst	XRF		N_2 physisorption							
	Si/Al	Co	S_{BET} $[m^2/g]^a$	S_{micro} $[m^2/g]^b$	S_{ext} $[m^2/g]^b$	V_{total} $[cm^3/g]^c$	V_{micro} $[cm^3/g]^b$	V_{meso} $[cm^3/g]^b$	IHF	Pore diameter $[nm]^d$
ZBU	53	–	417	197	220	0.10	0.08	0.02	0.89	2.25
2.5Co/ZBU	41	3	334	147	187	0.10	0.06	0.04	0.57	2.25
5Co/ZBU	41	8	372	190	181	0.07	0.07	0.00	0.64	2.25
10Co/ZBU	39	16	308	145	163	0.09	0.06	0.03	0.50	2.12
ZM	53	–	399	333	66	0.06	0.06	0.00	0.20	2.49
ZTD	51	–	382	200	182	0.11	0.08	0.04	0.74	2.51
2.5Co/ZTD	12	3	337	91	246	0.21	0.05	0.16	0.63	2.38
5Co/ZTD	23	9	346	126	220	0.23	0.06	0.17	0.67	2.64
10Co/ZTD	21	18	329	106	223	0.22	0.06	0.16	0.68	2.68

$$\text{IHF} = \left(\frac{V_{\text{micro}}}{V_{\text{micro,max}}}\right) \times \left(\frac{S_{\text{ext}}}{S_{\text{ext,max}}}\right) \quad (1)$$

A balanced presence of external porosity and well-preserved micropores is indicated by a high IHF value, whereas an imbalance favoring one pore type is suggested by a low IHF [48,49]. For instance, ZM sample with an abundant amount of microporous exhibited the lowest IHF value of 0.20. Among the hierarchical samples, pristine ZBU had a higher IHF (0.89) than ZTD (0.74), indicating a balanced amount of mesopores and micropores in the ZBU synthesized using dual-templating method. Cobalt incorporation led to varying IHF values; for ZBU samples the IHF value was in the order of 5Co/ZBU (0.64) > 2.5Co/ZBU (0.57) > 10Co/ZBU (0.50), while ZTD samples exhibited IHF values in the order of 10Co/ZTD (0.68) > 5Co/ZTD (0.67) > 2.5Co/ZTD (0.63). The observed changes in IHF values following Co incorporation indicate that Co-oxide modification alters the balance of hierarchical porosity in ZSM-5, as shown by the reduction in micropore volume and increase in mesopore volume. Such changes suggest that Co_3O_4 nanoparticles may partially block micropore entrances and simultaneously create 'mesoporosity' from interparticle voids resulting from stacked Co_3O_4 nanoparticles [43]. In that case, a variation of IHF values might also indicate the dispersion level of Co_3O_4 nanoparticles, with higher IHF values suggest better Co_3O_4 nanoparticles dispersion, as shown by 5Co/ZBU (0.64) and 10Co/ZTD (0.68). These variations underscore the distinct pore architectures resulting from the two synthesis strategies and their response to metal incorporation.

SEM analysis was employed to characterize the morphology and surface microstructure of the as-synthesized ZBU and ZTD catalysts, along with their Co-derivatives as shown in Figure 4 and Figure 5, respectively. The pristine ZM sample (Figure 5a) exhibited a smooth surface, indicative of its high crystallinity. In contrast, ZTD sample (Figure 5b) synthesized via desilication from ZM, largely retained its overall

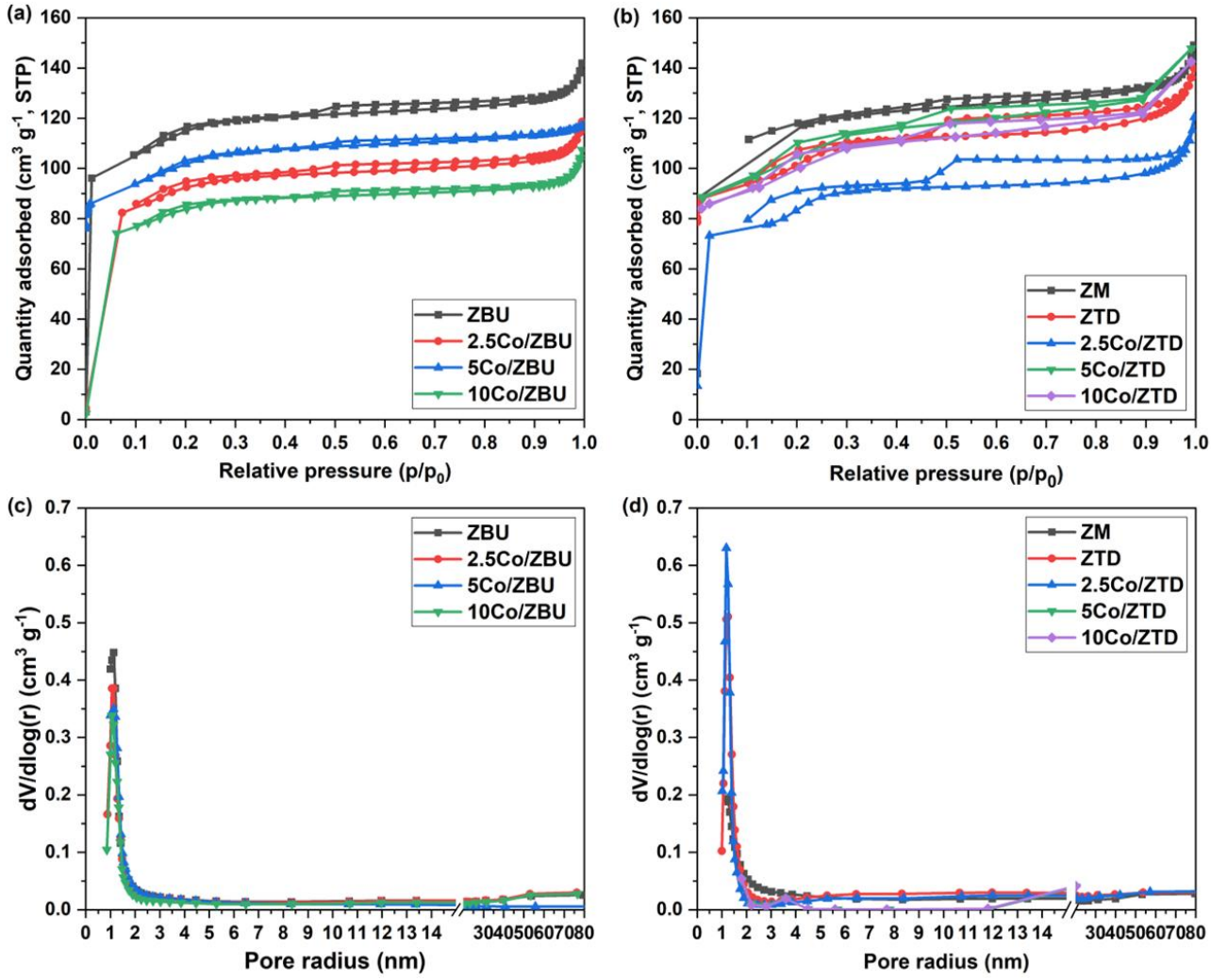

Figure 3. N_2 adsorption-desorption isotherm of (a) ZBU and (b) ZTD samples along with their Co_3O_4-derivatives, and BJH pore size distribution of (c) ZBU and (d) ZTD samples along with their Co_3O_4-derivatives.

hexagonal morphology but displayed a rougher surface. This increased surface roughness serves as an indication of the successful formation of mesopores through the desilication process. Similarly, ZBU sample synthesized via dual-templating method also presented a rough surface, confirming the formation of mesopores contributing to its hierarchical pore structure. ZBU (Figure 4a) exhibited a hexagonal coffin-like shape (500 nm), albeit with some visible surface irregularities or slight damage attributed to removal of secondary template (PDDA-Cl) under harsh condition of calcination process. Strong interactions between the zeolite crystals and this secondary template could lead to minor structural damage and the formation of mesopores upon its extraction from the ZSM-5 framework [50]. Conversely, ZTD sample (Figure 5b) also exhibited hexagonal morphology in smaller size compared to ZBU (3500 nm). However, the desilication treatment under alkaline solution resulted in a slightly uneven surface on the zeolite due to the extraction of Si atoms from the microporous ZSM-5 framework, which facilitates the formation of mesopores.

Upon the incorporation of Co-oxide, the overall morphology of both ZBU and ZTD catalysts remained largely unchanged, retaining their characteristic hexagonal morphology. Both Co/ZBU and Co/ZTD samples exhibited fine white crystals, indicative of Co-oxide nanoparticles deposited on the zeolite surface. The visible amount of Co-oxide nanoparticles increased proportionally with the higher amount of Cobalt loading, confirming the successful metal deposition. However, a notable difference in dispersion was observed, in which Co_3O_4 nanoparticles appeared to be more uniformly dispersed on the surface of ZTD samples compared to ZBU, where they tended to form more visually distinct particles. This suggests a better dispersion of the Co-oxide within the ZTD samples, which might be influenced by the unique surface characteristics resulting from the desilication process. These results confirmed the higher IHF values shown by ZTD samples, which are indicative of higher Co-oxide dispersion level on the surface of ZSM-5 [51].

3.2. Catalytic Test

The methane partial oxidation reaction was studied to determine the catalytic efficacy of the ZBU and ZTD Co-derivatives. The reactions were carried out in a batch reactor with a ratio of 0.75:2.00 bar CH_4 to N_2 (0.5% O_2) feedstock, respectively, at 150 °C for a reaction time of 60 minutes. These conditions are based on the prior research of our research group [18,19,52]. Each catalytic test was conducted as a single run to evaluate the immediate performance of the fresh catalyst sample.

Figure 6 illustrates the product yields obtained over all catalysts. Co/ZBU series exhibited total selectivity towards methanol, in which 5Co/ZBU demonstrated the highest methanol yield (62.08%), followed by 2.5Co/ZBU (19.86%), while 10Co/ZBU resulted in no detectable product. The decline in performance at higher Co-oxide loading, specifically for 10Co/ZBU, can be attributed to two main phenomena. Firstly, it might indicate the over-oxidation of CH_4 into CO_2, which is undetectable by our catalytic system. Secondly, and more significantly, it suggests the agglomeration of Co_3O_4 nanoparticles on the catalyst surface at higher metal concentrations. This agglomeration leads to pore blockage and a substantial reduction in available sites, thereby severely hindering catalytic efficiency [53]. The optimum Co-loading for the ZBU series was determined to be 5%.

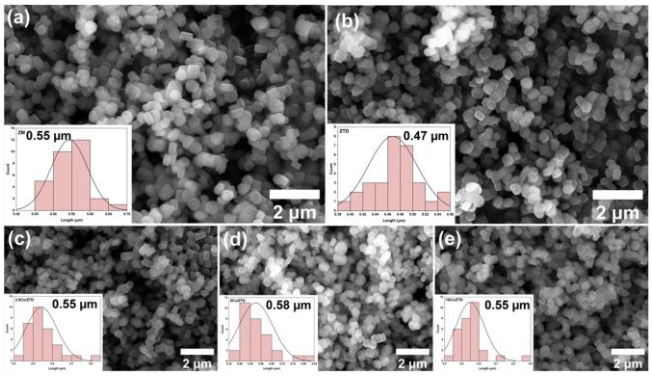

Figure 5. SEM images of (a) ZM, (b) ZTD, (c) 2.5Co/ZTD, (d) 5Co/ZTD, and (e) 10Co/ZTD (10,000x magnification, inset particle size distributions with an average particle size).

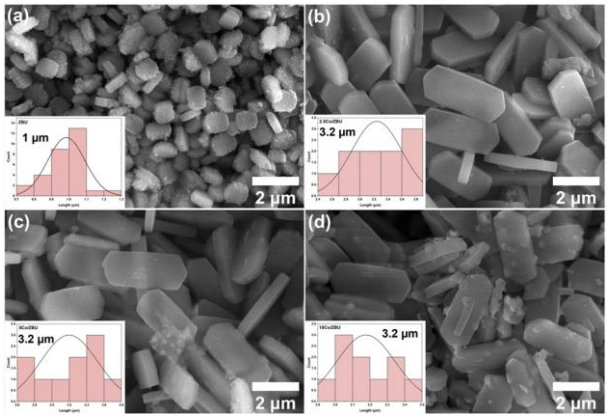

Figure 4. SEM images of (a) ZBU, (b) 2.5Co/ZBU, (c) 5Co/ZBU, and (d) 10Co/ZBU (10,000x magnification, inset particle size distributions with an average particle size).

In contrast, the ZTD catalyst series exhibited significantly lower yields compared to their ZBU counterparts. 2.5Co/ZTD yielded only a trace amount of methanol (0.02%), which was the highest for the ZTD series. 5Co/ZTD catalysts produced no detectable product, while 10Co/ZTD produced a small amount of formaldehyde (0.06%), suggesting further oxidation of intermediate products. The overall lower catalytic activity of the ZTD series, particularly for methanol production, can be linked to the desilication process, which leads to a decrease in the Si/Al ratio. This reduction in Si/Al ratio is known to affect the catalytic activity and stability of ZSM-5 catalyst [54,55]. The observed formaldehyde formation at higher Co loadings in ZTD could be due to increased acidity caused by desilication, which can promote selectivity towards formaldehyde. The optimum Co-loading for ZTD series was 2.5%.

These results obtained from this study highlight the importance of porosity in the application of ZSM-5 samples as catalysts in POM reaction. The ZBU series indicated better dispersion of Co_3O_4 on the ZSM-5 support, with lower pore diameter size compared to ZTD series. Therefore, ZBU series exhibited a better catalytic performance in terms of product yields. According to these findings, the best catalytic performance for partial oxidation of methane to methanol was verified, with ZTD exhibiting the greatest performance in its series at 2.5% Co loading and ZBU exhibiting the highest performance at 5% Co loading.

Table 2 presents a comprehensive comparison of the as-synthesized catalysts in this work with other reported catalysts for POM reaction. In this work, 5Co/ZBU catalyst achieved a remarkable 62.08% methanol yield, demonstrating competitive performance when compared to various Co/ZSM-5 and other zeolite-based catalysts in the literature. For instance, a previous study on Co/ZSM-5 (2024) reported a 74% methanol yield, albeit under different reaction conditions and likely with distinct synthesis methods impacting its properties. Other studies using SSZ-39 and various Co/ZSM-5 or Cu/ZSM-5 catalysts generally report yields in $\mu mol \cdot g cat^{-1}$ units, which are not directly comparable to our percentage yield but still indicate the high efficiency achieved in this work. This comparison underscores the effectiveness of our synthesized hierarchical Co_3O_4/ZSM-5 catalysts, particularly the ZBU variant, for direct methanol production via POM, positioning our work favorably within the current research landscape.

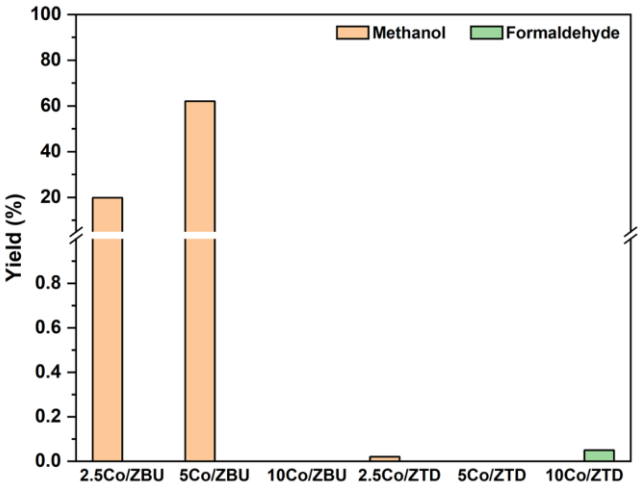

Figure 6. Catalytic activity in terms of product yields for the POM reaction from Co/ZBU and Co/ZTD samples.

4. Conclusions

This study successfully synthesized hierarchical ZSM-5 catalysts via both bottom-up (ZBU) and top-down (ZTD) methods, followed by cobalt oxide impregnation. Comprehensive characterization confirmed the integrity of the MFI framework while revealing distinct textural and morphological properties influenced by the synthesis route and Co incorporation. Pristine ZBU samples exhibited higher surface area compared to ZTD samples, while both catalysts demonstrated notable changes in pore volume balance upon Co incorporation, indicated by IHF variations. SEM confirmed coffin-like morphologies, with ZTD displaying a rougher surface and better Co-oxide dispersion compared to ZBU. In methane partial oxidation, the ZBU series demonstrated significantly superior catalytic performance. The 5% Co/ZBU catalyst achieved the highest methanol yield of 62.08%, while ZTD catalysts yielded considerably less, with 2.5% Co/ZTD producing only 0.02% methanol. The decline in yield at higher Co loadings (e.g., 10% Co/ZBU) was linked to Co-oxide agglomeration and pore blockage. The overall lower activity of the ZTD series stemmed from the desilication process, which reduced the Si/Al ratio, impacting catalytic stability and potentially promoting formaldehyde formation. These findings underscore the critical influence of the synthesis strategy on catalyst properties and their resultant performance in methane partial oxidation. Therefore, future work could focus on investigating the regeneration capabilities of these catalysts to ensure their long-term viability. Additionally, conducting long-term stability tests under continuous reaction conditions would be crucial to assess their durability and industrial applicability. Exploring the scale-up potential of these catalytic systems for larger-scale methane valorization processes also represents a promising direction.

Acknowledgments

This work was supported by the Indonesian Ministry of Research, Technology and Higher Education (Menristekdikti) through: (a) Pendidikan Magister menuju Doktor untuk Sarjana Unggul (PMDSU) Research Grant No. NKB-798/UN2.RST/HKP.05.00/2024 and (b) Beasiswa Peningkatan Kualitas Publikasi Internasional/Sandwich-like bagi Mahasiswa Penerima Beasiswa Pendidikan Magister menuju Doktor untuk Sarjana Unggul Research Grant No. 165.31/E4.4/KU/2023.

CRedit Author Statement

Author Contributions: Irena Khatrin: Formal analysis, Data curation, Writing – Original Draft, Visualization. Danika Nurranalya Putri: Validation, Formal analysis, Investigation, Data curation. Muhammad Ridwan: Methodology, Supervision. Yuni Krisyuningsih Krisnandi: Conceptualization, Methodology, Project administration, Writing – Review & Editing, Supervision, Funding acquisition. All authors have read and agreed to the published version of the manuscript.

References

[1] Dasireddy, V.D.B.C., Likozar, B. (2021). Direct methanol production from mixed methane/H2O/N2O feedstocks over Cu–Fe/Al2O3 catalysts. *Fuel*, 301. DOI: 10.1016/J.FUEL.2021.121084.

[2] Al-Ghussain, L. (2019). Global warming: review on driving forces and mitigation. *Environmental Progress & Sustainable Energy*, 38(1), 13–21. DOI: 10.1002/EP.13041.

[3] Litto, R., Hayes, R.E., Liu, B. (2007). Capturing fugitive methane emissions from natural gas compressor buildings. *Journal of Environmental Management*, 84(3), 347–361. DOI: 10.1016/J.JENVMAN.2006.06.007.

[4] Ravi, M., Ranocchiari, M., van Bokhoven, J.A. (2017). The Direct Catalytic Oxidation of Methane to Methanol—A Critical Assessment. *Angewandte Chemie International Edition*, 56(52), 16464–16483. DOI: 10.1002/ANIE.201702550.

[5] Kumar, A., Prasad, R., Sharma, Y.C. (2019). Ethanol steam reforming study over ZSM-5 supported cobalt versus nickel catalyst for renewable hydrogen generation. *Chinese Journal of Chemical Engineering*, 27(3), 677–684. DOI: 10.1016/J.CJCHE.2018.03.036.

[6] Smith, M.R., Ozkan, U.S. (1993). The Partial Oxidation of Methane to Formaldehyde: Role of Different Crystal Planes of MoO3. *Journal of Catalysis*, 141(1), 124–139. DOI: 10.1006/JCAT.1993.1124.

Table 2. Comparison of POM performance.

Catalyst	Properties		Reaction conditions		Methanol Yield	Formaldehyde Yield	Ref.
	Si/Al	S_{BET} [m^2/g][a]	Oxidant	Time (min)			
ZBU	53	417	0.5% O_2	60	–	–	This work
2.5Co/ZBU	41	334			19.86%	–	
5Co/ZBU	41	372			62.08%	–	
10Co/ZBU	39	308			–	–	
ZM	53	399			–	–	
ZTD	51	382			–	–	
2.5Co/ZTD	12	337			0.02%	–	
5Co/ZTD	23	346			–	–	
10Co/ZTD	21	329			–	0.06%	
Co/ZSM-5	59	317		30	74%	–	[19]
SSZ-39	–	452	O_2	200	9.82 ± 0.23 µmol $\cdot g_{cat}^{-1} \cdot h^{-1}$	–	[56]
Co/ZSM-5	–	0.24	O_2	25	1.0 µmol $\cdot g_{cat}^{-1}$	0.3 µmol $\cdot g_{cat}^{-1}$	[17]
Co/ZSM-5	–	–	O_2	25	0.39 µmol $\cdot g_{cat}^{-1}$	0.50 µmol $\cdot g_{cat}^{-1}$	[57]
Cu/ZSM-5	–	320	O_2	25	1.8 µmol $\cdot g_{cat}^{-1}$	–	[55]

[7] Spencer, N.D., Pereira, C.J. (1989). V2O5-SiO2-catalyzed methane partial oxidation with molecular oxygen. *Journal of Catalysis*, 116(2), 399–406. DOI: 10.1016/0021-9517(89)90106-1.

[8] Lyons, J.E., Ellis, P.E., Durante, V.A. (1991). Active Iron Oxo Centers for the Selective Catalytic Oxidation of Alkanes. *Studies in Surface Science and Catalysis*, 67(C), 99–116. DOI: 10.1016/S0167-2991(08)61930-8.

[9] Vadodaria, D.M., Al-Fatesh, A.S., Alrashed, M.M., Alhoshan, M., Ibrahim, A.A., Kumar, N.S., Kumar, R. (2025). A comprehensive review on catalytic oxidation of methane in the presence of molecular oxygen: total oxidation, partial oxidation and selective oxidation. *Catalysis Reviews*, 1–47. DOI: 10.1080/01614940.2025.2535991.

[10] Sudarsanam, P., Peeters, E., Makshina, E. V., Parvulescu, V.I., Sels, B.F. (2019). Advances in porous and nanoscale catalysts for viable biomass conversion. *Chemical Society Reviews*, 48(8), 2366–2421. DOI: 10.1039/C8CS00452H.

[11] Alanazi, R.S.A., Alreshaidan, S.B., Ibrahim, A.A., Wazeer, I., Alarifi, N., Bellahwel, O.A., Abasaeed, A.E., Al-Fatesh, A.S. (2025). Influence of Alumina and Silica Supports on the Performance of Nickel Catalysts for Methane Partial Oxidation. *Catalysts*, 15(2), 102. DOI: 10.3390/CATAL15020102/S1.

[12] Saha, D., Comroe, M., Krishna, R. (2021). Synthesis of Cu(I) doped mesoporous carbon for selective capture of ethylene from reaction products of oxidative coupling of methane (OCM). *Microporous and Mesoporous Materials*, 328, 111488. DOI: 10.1016/J.MICROMESO.2021.111488.

[13] Ma, L., Ding, C., Wang, J., Li, Y., Xue, Y., Guo, J., Zhang, K., Liu, P., Gao, X. (2019). Highly dispersed Pt nanoparticles confined within hierarchical pores of silicalite-1 zeolite via crystal transformation of supported Pt/S-1 catalyst for partial oxidation of methane to syngas. *International Journal of Hydrogen Energy*, 44(39), 21847–21857. DOI: 10.1016/J.IJHYDENE.2019.06.051.

[14] Dinh, K.T., Sullivan, M.M., Serna, P., Meyer, R.J., Dincă, M., Román-Leshkov, Y. (2018). Viewpoint on the Partial Oxidation of Methane to Methanol Using Cu- and Fe-Exchanged Zeolites. *ACS Catalysis*, 8(9), 8306–8313. DOI: 10.1021/ACSCATAL.8b01180.

[15] Singh, L., Rekha, P., Chand, S. (2018). Comparative evaluation of synthesis routes of Cu/zeolite Y catalysts for catalytic wet peroxide oxidation of quinoline in fixed-bed reactor. *Journal of Environmental Management*, 215, 1–12. DOI: 10.1016/J.JENVMAN.2018.03.021.

[16] Michalkiewicz, B. (2004). Partial oxidation of methane to formaldehyde and methanol using molecular oxygen over Fe-ZSM-5. *Applied Catalysis A: General*, 277(1–2), 147–153. DOI: 10.1016/J.APCATA.2004.09.005.

[17] Beznis, N. V., Van Laak, A.N.C., Weckhuysen, B.M., Bitter, J.H. (2011). Oxidation of methane to methanol and formaldehyde over Co–ZSM-5 molecular sieves: Tuning the reactivity and selectivity by alkaline and acid treatments of the zeolite ZSM-5 agglomerates. *Microporous and Mesoporous Materials*, 138(1–3), 176–183. DOI: 10.1016/J.MICROMESO.2010.09.009.

[18] Krisnandi, Y.K., Putra, B.A.P., Bahtiar, M., Zahara, Abdullah, I., Howe, R.F. (2015). Partial Oxidation of Methane to Methanol over Heterogeneous Catalyst Co/ZSM-5. *Procedia Chemistry*, 14, 508–515. DOI: 10.1016/J.PROCHE.2015.03.068.

[19] Khatrin, I., Abdullah, I., McCue, A.J., Krisnandi, Y.K. (2024). Mesoporous configuration effects on the physicochemical features of hierarchical ZSM-5 supported cobalt oxide as catalysts in methane partial oxidation. *Microporous and Mesoporous Materials*, 365, 112896. DOI: 10.1016/J.MICROMESO.2023.112896.

[20] Jia, X., Khan, W., Wu, Z., Choi, J., Yip, A.C.K. (2019). Modern synthesis strategies for hierarchical zeolites: Bottom-up versus top-down strategies. *Advanced Powder Technology*, 30(3), 467–484. DOI: 10.1016/J.APT.2018.12.014.

[21] Ogura, M., Shinomiya, S.Y., Tateno, J., Nara, Y., Kikuchi, E., Matsukata, M. (2000). Formation of Uniform Mesopores in ZSM-5 Zeolite through Treatment in Alkaline Solution. *Chemistry Letters*, 29(8), 882–883. DOI: 10.1246/CL.2000.882.

[22] Ahmad, K., Upadhyayula, S. (2019). Conversion of the greenhouse gas CO2 to methanol over supported intermetallic Ga–Ni catalysts at atmospheric pressure: thermodynamic modeling and experimental study. *Sustainable Energy & Fuels*, 3(9), 2509–2520. DOI: 10.1039/C9SE00165D.

[23] Syeitkhajy, A., Hamid, M.A., Boroglu, M.S., Boz, I. (2025). Efficient synthesis of phosphorus-promoted and alkali-modified ZSM-5 catalyst for catalytic dehydration of lactic acid to acrylic acid. *Results in Chemistry*, 13, 101942. DOI: 10.1016/J.RECHEM.2024.101942.

[24] Treacy, M.M.J., Higgins, J.B. (2007). ZSM-5, Calcined. *Collection of Simulated XRD Powder Patterns for Zeolites*, 278–279. DOI: 10.1016/B978-044453067-7/50604-3.

[25] Gille, T., Seifert, M., Marschall, M.S., Bredow, S., Schneider, T., Busse, O., Reschetilowski, W., Weigand, J.J. (2021). Conversion of Oxygenates on H-ZSM-5 Zeolites—Effects of Feed Structure and Si/Al Ratio on the Product Quality. *Catalysts*, 11(4), 432. DOI: 10.3390/CATAL11040432.

[26] Min, J.E., Kim, S., Kwak, G., Kim, Y.T., Han, S.J., Lee, Y., Jun, K.W., Kim, S.K. (2018). Role of mesopores in Co/ZSM-5 for the direct synthesis of liquid fuel by Fischer–Tropsch synthesis. *Catalysis Science & Technology*, 8(24), 6346–6359. DOI: 10.1039/C8CY01931B.

[27] Nada, M.H., Larsen, S.C. (2017). Insight into seed-assisted template free synthesis of ZSM-5 zeolites. *Microporous and Mesoporous Materials*, 239, 444–452. DOI: 10.1016/J.MICROMESO.2016.10.040.

[28] Liu, C.F., He, L.C., Wang, X.F., Chen, J., Lu, J.Q., Luo, M.F. (2022). Tailoring Co3O4 active species to promote propane combustion over Co3O4/ZSM-5 catalyst. *Molecular Catalysis*, 524, 112297. DOI: 10.1016/J.MCAT.2022.112297.

[29] Sridhar, A., Rahman, M., Infantes-Molina, A., Wylie, B.J., Borcik, C.G., Khatib, S.J. (2020). Bimetallic Mo-Co/ZSM-5 and Mo-Ni/ZSM-5 catalysts for methane dehydroaromatization: A study of the effect of pretreatment and metal loadings on the catalytic behavior. *Applied Catalysis A: General*, 589, 117247. DOI: 10.1016/J.APCATA.2019.117247.

[30] Zhang, J., Xiong, Z., Wei, J., Song, Y., Ren, Y., Xu, D., Lai, B. (2020). Catalytic ozonation of penicillin G using cerium-loaded natural zeolite (CZ): Efficacy, mechanisms, pathways and toxicity assessment. *Chemical Engineering Journal*, 383, 123144. DOI: 10.1016/J.CEJ.2019.123144.

[31] Guan, X., Duan, C., Wang, H., Lu, B., Zhao, J., Cai, Q. (2021). Tuneable oxidation of styrene to benzaldehyde and benzoic acid over Co/ZSM-5. *New Journal of Chemistry*, 45(38), 18192–18201. DOI: 10.1039/D1NJ03145G.

[32] Al-Jubouri, S.M. (2020). Synthesis of hierarchically porous ZSM-5 zeolite by self-assembly induced by aging in the absence of seeding-assistance. *Microporous and Mesoporous Materials*, 303, 110296. DOI: 10.1016/J.MICROMESO.2020.110296.

[33] Kostyniuk, A., Key, D., Mdleleni, M. (2020). 1-hexene isomerization over bimetallic M-Mo-ZSM-5 (M: Fe, Co, Ni) zeolite catalysts: Effects of transition metals addition on the catalytic performance. *Journal of the Energy Institute*, 93(2), 552–564. DOI: 10.1016/J.JOEI.2019.06.009.

[34] Howe, R.F. (2016). Synchrotron Infrared Spectroscopy of Microporous Materials. *Makara Journal of Science*, 20(2) DOI: 10.7454/MSS.V20I2.5950.

[35] Serrano, D.P., Pinnavaia, T.J., Aguado, J., Escola, J.M., Peral, A., Villalba, L. (2014). Hierarchical ZSM-5 zeolites synthesized by silanization of protozeolitic units: Mediating the mesoporosity contribution by changing the organosilane type. *Catalysis Today*, 227, 15–25. DOI: 10.1016/J.CATTOD.2013.10.052.

[36] Luo, W., Yang, X., Wang, Z., Huang, W., Chen, J., Jiang, W., Wang, L., Cheng, X., Deng, Y., Zhao, D. (2017). Synthesis of ZSM-5 aggregates made of zeolite nanocrystals through a simple solvent-free method. *Microporous and Mesoporous Materials*, 243, 112–118. DOI: 10.1016/J.MICROMESO.2017.01.040.

[37] Song, G., Chen, W., Dang, P., Yang, S., Zhang, Y., Wang, Y., Xiao, R., Ma, R., Li, F. (2018). Synthesis and Characterization of Hierarchical ZSM-5 Zeolites with Outstanding Mesoporosity and Excellent Catalytic Properties. *Nanoscale Research Letters*, 13(1), 1–13. DOI: 10.1186/S11671-018-2779-8.

[38] Sabarish, R., Unnikrishnan, G. (2017). Synthesis, characterization and catalytic activity of hierarchical ZSM-5 templated by carboxymethyl cellulose. *Powder Technology*, 320, 412–419. DOI: 10.1016/J.POWTEC.2017.07.041.

[39] Donaldson, P.M., Hawkins, A.P., Howe, R.F. (2025). Distinctive signatures and ultrafast dynamics of Brønsted sites, silanol nests and adsorbed water in zeolites revealed by 2D-IR spectroscopy. *Chemical Science*, 16(16), 6688–6704. DOI: 10.1039/D4SC08093A.

[40] Fan, C., Wu, Z., Li, Z., Qin, Z., Zhu, H., Dong, M., Wang, J., Fan, W. (2023). Controllable preparation of ultrafine Co3O4 nanoparticles on H-ZSM-5 with superior catalytic performance in lean methane combustion. *Fuel*, 334, 126815. DOI: 10.1016/J.FUEL.2022.126815.

[41] Ba Mohammed, B., Hsini, A., Abdellaoui, Y., Abou Oualid, H., Laabd, M., El Ouardi, M., Ait Addi, A., Yamni, K., Tijani, N. (2020). Fe-ZSM-5 zeolite for efficient removal of basic Fuchsin dye from aqueous solutions: Synthesis, characterization and adsorption process optimization using BBD-RSM modeling. *Journal of Environmental Chemical Engineering*, 8(5), 104419. DOI: 10.1016/J.JECE.2020.104419.

[42] Qiao, K., Zhou, F., Han, Z., Fu, J., Ma, H., Wu, G. (2019). Synthesis and physicochemical characterization of hierarchical ZSM-5: Effect of organosilanes on the catalyst properties and performance in the catalytic fast pyrolysis of biomass. *Microporous and Mesoporous Materials*, 274, 190–197. DOI: 10.1016/J.MICROMESO.2018.07.028.

[43] Chen, K., Zhang, T., Chen, X., He, Y., Liang, X. (2018). Model construction of micro-pores in shale: A case study of Silurian Longmaxi Formation shale in Dianqianbei area, SW China. *Petroleum Exploration and Development*, 45(3), 412–421. DOI: 10.1016/S1876-3804(18)30046-6.

[44] Octaviani, S., Krisnandi, Y.K., Abdullah, I., Sihombing, R. (2012). The Effect of Alkaline Treatment to the Structure of ZSM5 Zeolites. *Makara Journal of Science*, 16(3), 155–162. DOI: 10.7454/mss.v16i3.1476/Makara.

[45] Liu, C., Chen, Y., Zhao, Y., Lyu, S., Wei, L., Li, X., Zhang, Y., Li, J. (2020). Nano-ZSM-5-supported cobalt for the production of liquid fuel in Fischer-Tropsch synthesis: Effect of preparation method and reaction temperature. *Fuel*, 263, 116619. DOI: 10.1016/J.FUEL.2019.116619.

[46] Kadja, G.T.M., Suprianti, T.R., Ilmi, M.M., Khalil, M., Mukti, R.R., Subagjo (2020). Sequential mechanochemical and recrystallization methods for synthesizing hierarchically porous ZSM-5 zeolites. *Microporous and Mesoporous Materials*, 308 DOI: 10.1016/J.MICROMESO.2020.110550.

[47] Khatrin, I., Kusuma, R.H., Kadja, G.T.M., Krisnandi, Y.K. (2023). Significance of ZSM-5 hierarchical structure on catalytic cracking: Intra- vs inter-crystalline mesoporosity. *Inorganic Chemistry Communications*, 149, 110447. DOI: 10.1016/J.INOCHE.2023.110447.

[48] Verboekend, D., Mitchell, S., Milina, M., Groen, J.C., Pérez-Ramírez, J. (2011). Full compositional flexibility in the preparation of mesoporous MFI zeolites by desilication. *Journal of Physical Chemistry C*, 115(29), 14193–14203. DOI: 10.1021/JP201671S.

[49] Bonilla, A., Baudouin, D., Pérez-Ramírez, J. (2009). Desilication of ferrierite zeolite for porosity generation and improved effectiveness in polyethylene pyrolysis. *Journal of Catalysis*, 265(2), 170–180. DOI: 10.1016/J.JCAT.2009.04.022.

[50] Sang, S., Chang, F., Liu, Z., He, C., He, Y., Xu, L. (2004). Difference of ZSM-5 zeolites synthesized with various templates. *Catalysis Today*, 93–95, 729–734. DOI: 10.1016/J.CATTOD.2004.06.091.

[51] Zhu, Z., Lu, G., Zhang, Z., Guo, Y., Guo, Y., Wang, Y. (2013). Highly active and stable Co3O4/ZSM-5 catalyst for propane oxidation: Effect of the preparation method. *ACS Catalysis*, 3(6), 1154–1164. DOI: 10.1021/CS400068V.

[52] Krisnandi, Y.K., Nurani, D.A., Alfian, D. V., Sofyani, U., Faisal, M., Saragi, I.R., Pamungkas, A.Z., Pratama, A.P. (2021). The new challenge of partial oxidation of methane over Fe2O3/NaY and Fe3O4/NaY heterogeneous catalysts. *Heliyon*, 7(11). DOI: 10.1016/j.heliyon.2021.e08305.

[53] Ghaedi, M., Izadbakhsh, A. (2021). Effects of Ca content on the activity of HZSM-5 nanoparticles in the conversion of methanol to olefins and coke formation. *Ranliao Huaxue Xuebao/Journal of Fuel Chemistry and Technology*, 49(10), 1468–1486. DOI: 10.1016/S1872-5813(21)60130-5.

[54] An, B., Li, Z., Wang, Z., Zeng, X., Han, X., Cheng, Y., Sheveleva, A.M., Zhang, Z., Tuna, F., McInnes, E.J.L., Frogley, M.D., Ramirez-Cuesta, A.J., S. Natrajan, L., Wang, C., Lin, W., Yang, S., Schröder, M. (2022). Direct photo-oxidation of methane to methanol over a mono-iron hydroxyl site. *Nature Materials 2022 21:8*, 21(8), 932–938. DOI: 10.1038/s41563-022-01279-1.

[55] Beznis, N.V., Weckhuysen, B.M., Bitter, J.H. (2010). Cu-ZSM-5 zeolites for the formation of methanol from methane and oxygen: Probing the active sites and spectator species. *Catalysis Letters*, 138(1–2), 14–22. DOI: 10.1007/S10562-010-0380-6.

[56] Pokhrel, J., Shantz, D.F. (2023). Continuous partial oxidation of methane to methanol over Cu-SSZ-39 catalysts. *Journal of Catalysis*, 421, 300–308. DOI: 10.1016/J.JCAT.2023.03.021.

[57] Beznis, N.V., Weckhuysen, B.M., Bitter, J.H. (2010). Partial oxidation of methane over Co-ZSM-5: Tuning the oxygenate selectivity by altering the preparation route. *Catalysis Letters*, 136(1–2), 52–56. DOI: 10.1007/S10562-009-0206-6.